Water Oxidation

DOI: 10.1002/anie.201406540

Water Oxidation Catalyzed by a Dinuclear Cobalt–Polypyridine Complex**

Hong-Yan Wang, Edgar Mijangos, Sascha Ott, and Anders Thapper**

Abstract: *The dinuclear Co complex [(TPA)Co(μ-OH)(μ-O_2)Co(TPA)]$(ClO_4)_3$ (**1**, TPA = tris(2-pyridylmethyl)amine) catalyzes the oxidation of water. In the presence of [Ru(bpy)$_3$]$^{2+}$ and $S_2O_8^{2-}$, photoinduced oxygen evolution can be observed with a turnover frequency (TOF) of 1.4 ± 0.1 mol(O_2) mol(**1**)$^{-1}$ s^{-1} and a maximal turnover number (TON) of 58 ± 5 mol(O_2) mol(**1**)$^{-1}$. The complex is shown to act as a molecular and homogeneous catalyst and a mechanism is proposed based on the combination of EPR data and light-driven O_2 evolution kinetics.*

The development of molecular catalysts for water oxidation based on abundant first row transition metals is central to future renewable solar fuel schemes.[1] An appealing strategy to lowering the energy demand of this process is to use multinuclear transition metal catalysts which enable storage of the oxidation equivalents necessary for water oxidation distributed over several metal centers.[2] This strategy is similar to what nature uses in the water-oxidizing complex in PSII.[3] In this context, multinuclear Co complexes, Co_4O_4-cubanes,[4] and tetracobalt polyoxometallates,[5] have been reported as homogeneous catalysts for water oxidation in chemical oxidation and photoinduced systems. On the other hand, molecular Co-based water oxidation catalysts with organic ligands have hitherto almost exclusively been limited to mononuclear complexes.[6] The only exception is a report of electrochemical water oxidation with two complexes that use bispyridylpyrazolate (bpp) as a bridging ligand between the Co ions.[7] Catalysis was, however, performed in acidic conditions (pH 2.1) and the catalysts were reported to have more than 700 mV overpotential for water oxidation.

Herein, we present a dinuclear cobalt complex [(TPA)Co(μ-OH)(μ-O_2)Co(TPA)]$(ClO_4)_3$ (**1**; TPA = tris(2-pyridylmethyl)amine) as a molecular and homogenous catalyst for electrochemical and photochemical water oxidation. Complex **1** has an overpotential for water oxidation of 540 mV at near neutral conditions (pH 8), and can catalyze oxygen evolution assisted by a photosensitizer, [Ru(bpy)$_3$]$^{2+}$, and an electron acceptor, $Na_2S_2O_8$, under visible-light irradiation. The possibility to use the catalyst for photoinduced O_2 evolution is important and crucial for applications in artificial photosynthesis.[2,8] A combination of UV/Vis, dynamic light scattering (DLS), and electron paramagnetic resonance (EPR) measurements identifies **1** as a molecular catalyst for water oxidation, and allows a mechanistic proposal for the catalyst's mode of action.

The dinuclear Co complex **1** was obtained as a brown powder through oxidation of [Co(TPA)Cl]Cl[9] by molecular oxygen in an aqueous solution (Scheme 1). ESI-MS peaks at

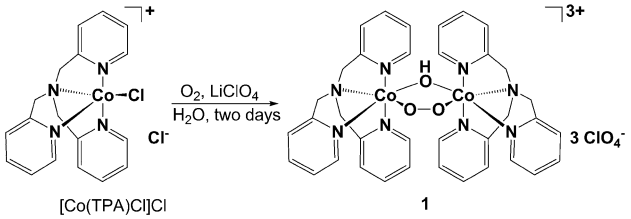

Scheme 1. Synthesis of [(TPA)Co(μ-OH)(μ-O_2)Co(TPA)]$(ClO_4)_3$ (**1**).

m/z = 372.2 ([M^{3+} − H^+]/2) and 248.4 ([M^{3+}]/3) confirm the dinuclear $Co^{III}Co^{III}$ structure of **1** in solution. The UV/Vis absorption spectrum of **1** exhibits a band at ca. 390 nm and a shoulder at ca. 470 nm, both in CH_3CN and water solution, supporting the notion that the dinuclear structure of **1** is retained in the two solvents (Figure S1).

Vapor diffusion of Et_2O into a CH_3CN solution of **1** yielded dark brown crystals suitable for X-ray diffraction. The molecular structure of **1** is shown in Figure 1. The structure consists of two Co^{III} ions with distorted octahedral geometry, bridged by a μ-OH and a μ-O_2 bridge, each with a TPA ligand coordinating all four nitrogen donor atoms to its

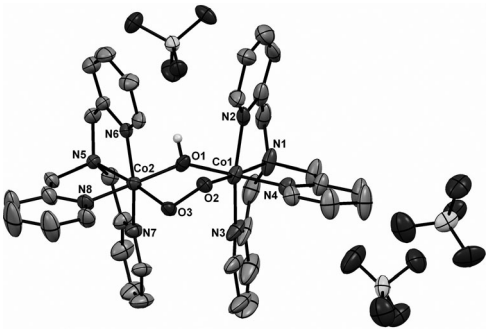

Figure 1. Crystal structure of **1** (ellipsoids at 50% probability level).

[*] Dr. H.-Y. Wang
School of Chemistry and Chemical Engineering
Shaanxi Normal University
Xi'an 710062 (P. R. China)
Dr. H.-Y. Wang, Dr. E. Mijangos, Dr. S. Ott, Dr. A. Thapper
Department of Chemistry—Ångström Laboratory
Uppsala University
P.O. Box 523, 75120 Uppsala (Sweden)
E-mail: anders.thapper@kemi.uu.se

[**] This work was supported by grants from the Swedish Energy Agency and the Knut and Alice Wallenberg Foundation.

Supporting information for this article is available on the WWW under http://dx.doi.org/10.1002/anie.201406540.

metal center. The doubly bridging μ-OH/μ-O_2 motif has been observed in other cobalt complexes[10] and is suggested to enhance the kinetic stability of the compounds. The Co–Co distance in **1** is 3.265 Å, and the O2–O3 bond is 1.412 Å, which is in the typical peroxo range of 1.4–1.5 Å.[10d]

Characterization of **1** by cyclic voltammetry in CH_3CN under an Ar atmosphere with nBu$_4$NPF$_6$ as electrolyte displays a reversible Co-based oxidation at 1.34 V (versus normal hydrogen electrode, NHE) and an irreversible reduction at −0.20 V (Figure S2). Controlled potential electrolysis indicates that the oxidation at 1.34 V (Figure S3) is a one-electron process ($Co^{III}Co^{III} \rightarrow Co^{IV}Co^{III}$). An EPR spectrum of an aliquot from the bulk electrolysis shows a signal centered at $g = 2.03$ that is very similar to the EPR signals of two reported dinuclear peroxo-bridged $Co^{IV}Co^{III}$ complexes[7,10d] (Figure S4). The reductive process at −0.20 V is assigned to a $Co^{III}Co^{III}/Co^{II}Co^{III}$ couple.

In borate buffer (pH 8) the complex shows a very different electrochemical response. The oxidation is observed at 1.05 V, and is followed directly by a catalytic wave for water oxidation (Figure 2). The cathodic shift in oxidation potential

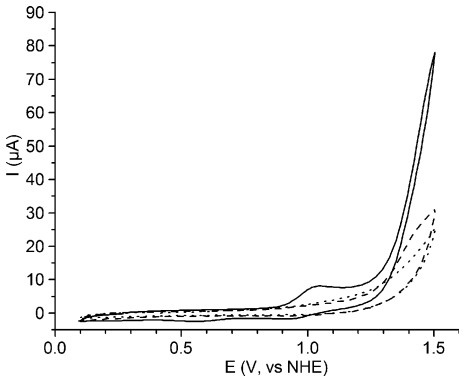

Figure 2. Cyclic voltammetry of **1** (0.5 mM, solid line) in 0.1 M borate buffer (pH 8), and the buffer alone (dotted line) at a scan rate of 100 mV s^{-1} under Ar atmosphere with a 3 mm glassy carbon working electrode, a glassy carbon rod counter electrode, and a Ag/AgCl (with saturated KCl aqueous solution) reference electrode. After a short bulk electrolysis (10 s) of **1** at 1.31 V the working electrode was placed again in fresh buffer (dashed line) and showed no catalytic water oxidation wave.

can be rationalized by deprotonation of the hydroxy bridge in borate buffer at pH 8. An experiment to reproduce this shift in CH_3CN solution by addition of a base, 2,6-lutidine, to **1** causes a slight shift (≈ 50 mV) in the redox potential of the $Co^{IV}Co^{III}/Co^{III}Co^{III}$ couple (Figure S2). Interestingly, a second oxidation process with a peak potential of ca. 1.7 V is also observed. We assign this to the oxidation of deprotonated $Co^{IV}Co^{III}$ dimer to the $Co^{IV}Co^{IV}$ state. This result exemplifies charge equilibration through deprotonation to access higher oxidation states of the catalyst.

The onset of the catalytic wave in borate buffer is around 1.30 V which gives an overpotential of 540 mV for water oxidation catalyzed by **1**.[11] This overpotential is lower than that of the previously reported dinuclear Co complexes and in the range of reported overpotentials for mononuclear Co complexes (300–600 mV).[6a,d,e] Importantly, both the oxidation and the catalytic wave occur at a low enough potential to be thermodynamically accessible by photogenerated [Ru(bpy)$_3$]$^{3+}$ oxidant ($E_{ox} = 1.3$ V vs. NHE).[9] After a short controlled potential electrolysis (10 s) of **1** at 1.3 V no deposition was observed on the working electrode and the CV in fresh buffer showed no catalytic water oxidation wave (Figure 2) confirming that the electrochemical response was originating from **1** in solution.

To investigate whether **1** could act as a catalyst for light-driven water oxidation, a borate-buffered solution containing **1**, [Ru(bpy)$_3$](ClO$_4$)$_2$, and $Na_2S_2O_8$ was irradiated with visible light and oxygen evolution was measured in a Clark electrode. Under irradiation, oxygen evolution starts after a lag phase of about 3 s and during the first 30 s, the amount of O_2 increases linearly.[12] After ca. 60 s, the concentration of oxygen is no longer increasing (Figure 3). A pH of 8 was found optimal for

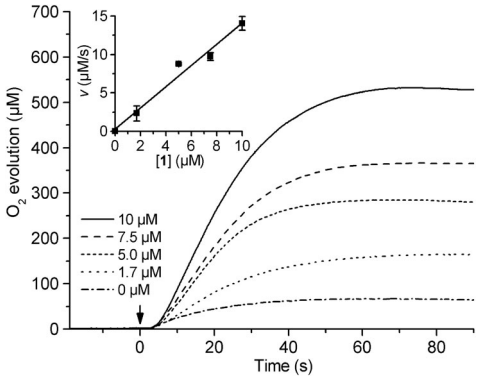

Figure 3. Light-induced water oxidation in a 1 mL reaction containing **1** (0, 1.7 μM, 5.0 μM, 7.5 μM, and 10 μM), [Ru(bpy)$_3$](ClO$_4$)$_2$ (0.4 mM), and $Na_2S_2O_8$ (3 mM) in borate buffer (50 mM, pH 8). The Clark cell was kept constant at 20 °C, and the system was irradiated using LEDs ($\lambda = 470 \pm 10$ nm, 820 μE cm^{-2} s^{-1}). The arrow indicates the start of the irradiation. Inset: plot of oxygen evolution initial velocities (v) versus [**1**]. The rate, v, is calculated in the linear part during the first 15 s of illumination and corrected for v when [**1**] = 0.

the process (see Table S1) as a lower pH renders photocatalysis much less efficient, whereas higher pH values give rise to increased initial oxygen evolution rates, but also faster deactivation with overall lower TONs. Figure 3 and Table 1 show the effect of varying the concentration of **1** in 50 mM borate buffer at the optimal pH. The control experiment with a combination of [Ru(bpy)$_3$](ClO$_4$)$_2$ and $Na_2S_2O_8$ in the absence of **1** produces only a small amount of O_2, and it is thus clear that **1** is required for efficient water oxidation (Figure 3). For 1.7 μM **1**, the O_2 concentration reaches about 164 μM after 60 s of irradiation, equivalent to a TON of 58 mol(O_2) mol(**1**)$^{-1}$ (corrected for the background oxygen evolution activity). Increasing the concentration of **1** gave more O_2, however, at the cost of gradually decreasing TONs. A plot of the rates (v) for oxygen evolution versus [**1**] is linear, giving a rate constant $k = 1.4 \pm 0.1$ s^{-1} at 20 °C. The first-order behavior with regard to [**1**] suggests a unimolecular reaction as the rate-determining step for oxygen evolution catalyzed by **1**, similar to what was found for the water oxidation

Table 1: O_2 evolution, TON, and TOF (corrected for background oxygen evolution activity) for different concentrations of **1**.

[**1**] [μM]	c_{O_2} [μM]	TON [mol(O_2) mol(**1**)$^{-1}$]	TOF [mol(O_2) (mol(**1**) s)$^{-1}$]
0	66 ± 5	–	–
1.7	164 ± 10	58 ± 5	1.4 ± 0.6
5	285 ± 9	44 ± 2	1.75 ± 0.03
7.5	367 ± 26	40 ± 4	1.30 ± 0.07
10	534 ± 4	47 ± 1	1.41 ± 0.09

catalyst $[(Ru^{II}(tpy)(H_2O))_2(\mu\text{-bpp})]^{3+}$, where the critical O–O bond formation step has been proposed to involve an intramolecular O···O interaction.[13] The intramolecular O–O bond formation is in contrast with one of the recently reported mononuclear Co complexes,[6f] and another dinuclear Ru complex,[14] for which an intermolecular interaction was proposed for the O–O bond formation step.

The molecular integrity of **1** during photocatalysis was scrutinized by dynamic light scattering (DLS) experiments. This method can identify the potential formation of CoO_x nanoparticles down to a size of about 1 nm which could be alternative catalysts for water oxidation.[15] In a sample that has been illuminated for 60 seconds, there is no evidence of any light scattering that would arise from CoO_x particle formation, suggesting that no Co oxide colloids are formed during the illumination (Figure S5).[15c] A further line of evidence for the molecular nature of the catalyst is based on an attempted recycling experiment in which $[Ru(bpy)_3]^{2+}$ and $Na_2S_2O_8$ were added to the illumination experiment when oxygen evolution had ceased (after 100 s). Renewed oxygen evolution can be detected, but only near the background activity found in the absence of **1** (Figure S6 black). Control experiments with $Co(ClO_4)_2$, that is known to form CoO_x under oxidizing conditions and to act as a water oxidation catalyst,[15c,16] give different results, because 1) DLS shows the formation of large particles (Figure S5c) and 2) 74% of the initial activity is retained after a second addition of fresh $Na_2S_2O_8$ and $Ru(bpy)_3(ClO_4)_2$ (Figure S6 red). Together, these observations show that **1** does not form CoO_x particles under the reaction conditions used during illumination and confirm that the catalyst for water oxidation is in fact **1**.

EPR spectroscopy was employed as a spectroscopic tool to acquire further insights into the catalytic mechanism, analyzing samples before and after irradiation using 532 nm laser flashes. A mixture of **1**, $[Ru(bpy)_3]^{2+}$, and $S_2O_8^{2-}$ in borate buffer (pH 8) is EPR-silent before illumination, consistent with the expected $Co^{III}Co^{III}$ ground state of **1**. After one laser flash, the EPR spectrum at 10 K shows a signal at $g = 2.03$ (Figure 4) that is very similar to that found after bulk electrolysis in MeCN and that is therefore assigned to a low spin $S = {}^1/_2$ mixed-valent $Co^{III}Co^{IV}$ species.[7,10d] This is the same EPR-signal that is obtained when **1** is chemically oxidized by $[Ru(bpy)_3]^{3+}$ in 1:1 borate buffer/CH_3CN solution (Figure S7).

Applying more laser flashes leads to a gradual decrease of the $Co^{III}Co^{IV}$ signal, and the emergence

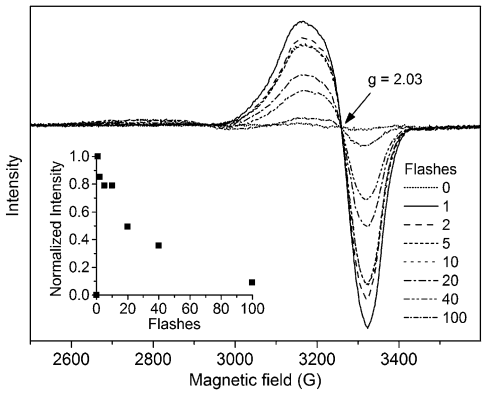

Figure 4. EPR spectra of a mixture containing **1** (52 μM), $[Ru(bpy)_3](ClO_4)_2$ (0.3 mM), and $Na_2S_2O_8$ (2.25 mM) in borate buffer (50 mM, pH 8) after 0, 1, 2, 5, 10, 20, 40, and 100 laser flashes (532 nm, 6 ns, 4 W). The samples were frozen within 5 s after the illumination. Inset: The intensity of the EPR signal centered at $g = 2.03$ versus the number of flashes. EPR parameters; $T = 10$ K; microwave power = 20 μW; microwave frequency = 9.28 GHz.

of broad spectral features ranging from 2500 to 2950 G (Figure S8). This broad signal has contributions from at least two components, one with a peak centered at about 2750 G ($g = 2.42$) and one at about 2825 G ($g = 2.33$). EPR signals with $g_{eff} \approx 2.3$ were recently reported as a spectroscopic evidence for $Co^{IV}(O)$ species in Co oxide films,[17] as well as in a $Co^{III}{}_3Co^{IV}O_4$ cubane.[18] As complex **1** does not form any higher CoO_x clusters or particles (see above), it is tempting to propose that the $g = 2.33$ signal originates from a $Co^{IV}(O)$ species involved in the catalytic cycle of **1**. The EPR signal at $g = 2.42$ may arise from a Ru^{III} species that stems from decomposition of the photosensitizer as it can also be observed in a control illumination experiment in the absence of **1** (Figure S8). However, both signals are very weak and an unambiguous assignment of the $g = 2.33$ signal to a Co^{IV} species is not possible from this experiment. Other methods for characterizing this potential Co^{IV} intermediate are currently pursued.

Based on the experimental data the following mechanism for water oxidation catalyzed by **1** is proposed (Scheme 2). The first oxidation of the $Co^{III}Co^{III}$ complex (**1**) by photooxidized $[Ru(bpy)_3]^{3+}$ produces an EPR active peroxo-

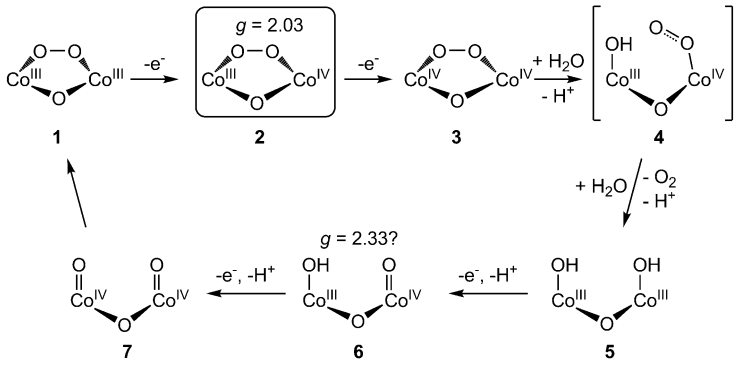

Scheme 2. Proposed mechanism for water oxidation catalyzed by **1**. Only the center of the complex is shown.

bridged $Co^{III}Co^{IV}$ complex (**2**) that is characterized by the $g = 2.03$ signal. The second oxidation gives rise to an antiferromagnetically coupled EPR-silent peroxo-bridged $Co^{IV}Co^{IV}$ complex (**3**), that has also been proposed for other Co-based catalysts.[6f] This species releases O_2 through the sequential addition of two water molecules giving a $(OH)Co^{III}Co^{III}(OH)$ species (**5**).[17b,19] Further oxidation of **5** and deprotonation results in a $(OH)Co^{III}Co^{IV}(O)$ species (**6**) that contains a $Co^{IV}(O)$ moiety similar to that found in studies of CoO_x.[17] A second oxidation and deprotonation produces a reactive $(O)Co^{IV}Co^{IV}(O)$ species (**7**) that undergoes intramolecular O–O bond formation to close the catalytic cycle. Intramolecular O–O bond formation from **7** to the starting complex **1** has previously been proposed for another dinuclear Co complex,[7] and was further suggested in a theoretical study of a Co cubane.[19] It should be pointed out that the O–O bond could as well form through a water nucleophilic attack on one of the $Co^{IV}(O)$ groups.[17b,20] However, theoretical calculations indicate that the water nucleophilic attack on the oxidized $Co^{IV}O$ group requires the formation of a $Co^{IV}O^{\bullet}$ state, formally a Co^{V} state,[20] that lacks any experimental evidence of its existence during water oxidation.

In summary, a dinuclear Co complex **1** has been prepared and was shown to catalyze the oxidation of water at near neutral conditions (pH 8) as the first molecular dinuclear catalyst for effective photo-driven water oxidation. The first oxidation step in the proposed catalytic cycle has been followed both photochemically and electrochemically. In addition, a second oxidation step becomes accessible through charge equilibration by deprotonation in nonaqueous medium. Investigations to further identify active intermediates in the catalytic cycle to increase the mechanistic understanding of the process are ongoing.

Received: June 24, 2014
Published online: October 27, 2014

Keywords: dinuclear cobalt complexes · homogeneous catalysis · photocatalysis · water oxidation

[1] a) P. Du, R. Eisenberg, *Energy Environ. Sci.* **2012**, *5*, 6012 – 6021; b) H. Yamazaki, A. Shouji, M. Kajita, M. Yagi, *Coord. Chem. Rev.* **2010**, *254*, 2483 – 2491; c) V. Artero, M. Chavarot-Kerlidou, M. Fontecave, *Angew. Chem. Int. Ed.* **2011**, *50*, 7238 – 7266; *Angew. Chem.* **2011**, *123*, 7376 – 7405.

[2] A. Sartorel, M. Bonchio, S. Campagna, F. Scandola, *Chem. Soc. Rev.* **2013**, *42*, 2262 – 2280.

[3] H. Dau, M. Haumann, *Coord. Chem. Rev.* **2008**, *252*, 273 – 295.

[4] a) S. Berardi, G. La Ganga, M. Natali, I. Bazzan, F. Puntoriero, A. Sartorel, F. Scandola, S. Campagna, M. Bonchio, *J. Am. Chem. Soc.* **2012**, *134*, 11104 – 11107; b) N. S. McCool, D. M. Robinson, J. E. Sheats, G. C. Dismukes, *J. Am. Chem. Soc.* **2011**, *133*, 11446 – 11449; c) F. Evangelisti, R. Guttinger, R. More, S. Luber, G. R. Patzke, *J. Am. Chem. Soc.* **2013**, *135*, 18734 – 18737.

[5] a) Q. Yin, J. M. Tan, C. Besson, Y. V. Geletii, D. G. Musaev, A. E. Kuznetsov, Z. Luo, K. I. Hardcastle, C. L. Hill, *Science* **2010**, *328*, 342 – 345; b) N. Planas, L. Vigara, C. Cady, P. Miró, P. Huang, L. Hammarström, S. Styring, N. Leidel, H. Dau, M. Haumann, L. Gagliardi, C. J. Cramer, A. Llobet, *Inorg. Chem.* **2011**, *50*, 11134 – 11142.

[6] a) D. K. Dogutan, R. McGuire, Jr., D. G. Nocera, *J. Am. Chem. Soc.* **2011**, *133*, 9178 – 9180; b) C.-F. Leung, S.-M. Ng, C.-C. Ko, W.-L. Man, J. Wu, L. Chen, T.-C. Lau, *Energy Environ. Sci.* **2012**, *5*, 7903 – 7907; c) S. Tanaka, M. Annaka, K. Sakai, *Chem. Commun.* **2012**, *48*, 1653 – 1655; d) D. J. Wasylenko, R. D. Palmer, E. Schott, C. P. Berlinguette, *Chem. Commun.* **2012**, *48*, 2107 – 2109; e) E. Pizzolato, M. Natali, B. Posocco, A. Montellano Lopez, I. Bazzan, M. Di Valentin, P. Galloni, V. Conte, M. Bonchio, F. Scandola, A. Sartorel, *Chem. Commun.* **2013**, *49*, 9941 – 9943; f) T. Nakazono, A. R. Parent, K. Sakai, *Chem. Commun.* **2013**, *49*, 6325 – 6327.

[7] M. L. Rigsby, S. Mandal, W. Nam, L. C. Spencer, A. Llobet, S. S. Stahl, *Chem. Sci.* **2012**, *3*, 3058 – 3062.

[8] A. Magnuson, M. Anderlund, O. Johansson, P. Lindblad, R. Lomoth, T. Polivka, S. Ott, K. Stensjö, S. Styring, V. Sundström, L. Hammarström, *Acc. Chem. Res.* **2009**, *42*, 1899 – 1909.

[9] H. Wang, Y. Lu, E. Mijangos, A. Thapper, *Chin. J. Chem.* **2014**, *32*, 467 – 473.

[10] a) R. F. Bogucki, G. McLendon, A. E. Martell, *J. Am. Chem. Soc.* **1976**, *98*, 3202 – 3205; b) R. MacArthur, A. Sucheta, F. F. Chong, O. Einarsdóttir, *Proc. Natl. Acad. Sci. USA* **1995**, *92*, 8105 – 8109; c) C. Ludovici, R. Fröhlich, K. Vogtt, B. Mamat, M. Lübben, *Eur. J. Biochem.* **2002**, *269*, 2630 – 2637; d) Y. I. Cho, D. M. Joseph, M. J. Rose, *Inorg. Chem.* **2013**, *52*, 13298 – 13300.

[11] The potential for the onset of the catalytic wave is taken as the point at which the current is twice that of the irreversible oxidation wave. The potential for water oxidation at pH 8 is 0.76 V vs. NHE ($1.23 - 0.059 \times 8$ V).

[12] This lag phase has been observed by us before (see Ref. [15c]) and can be attributed to the build-up of Ru^{III} before oxygen evolution starts. When $[Ru(bpy)_3]^{3+}$ is added as a chemical oxidant the oxygen evolution starts within 1 s which is the response time of the electrode.

[13] S. Romain, F. Bozoglian, X. Sala, A. Llobet, *J. Am. Chem. Soc.* **2009**, *131*, 2768 – 2769.

[14] S. Maji, L. Vigara, F. Cottone, F. Bozoglian, J. Benet-Buchholz, A. Llobet, *Angew. Chem. Int. Ed.* **2012**, *51*, 5967 – 5970; *Angew. Chem.* **2012**, *124*, 6069 – 6072.

[15] a) G. L. Elizarova, G. M. Zhidomirov, V. N. Parmon, *Catal. Today* **2000**, *58*, 71 – 88; b) O. V. Gerasimov, G. L. Elizarova, V. N. Parmon, *J. Photochem. Photobiol. B* **1992**, *13*, 335 – 338; c) D. Shevchenko, M. F. Anderlund, A. Thapper, S. Styring, *Energy Environ. Sci.* **2011**, *4*, 1284 – 1287.

[16] H. Y. Wang, J. Liu, J. Zhu, S. Styring, S. Ott, A. Thapper, *Phys. Chem. Chem. Phys.* **2014**, *16*, 3661 – 3669.

[17] a) J. G. McAlpin, Y. Surendranath, M. Dinca, T. A. Stich, S. A. Stoian, W. H. Casey, D. G. Nocera, R. D. Britt, *J. Am. Chem. Soc.* **2010**, *132*, 6882 – 6883; b) J. B. Gerken, J. G. McAlpin, J. Y. Chen, M. L. Rigsby, W. H. Casey, R. D. Britt, S. S. Stahl, *J. Am. Chem. Soc.* **2011**, *133*, 14431 – 14442.

[18] J. G. McAlpin, T. A. Stich, C. A. Ohlin, Y. Surendranath, D. G. Nocera, W. H. Casey, R. D. Britt, *J. Am. Chem. Soc.* **2011**, *133*, 15444 – 15452.

[19] L.-P. Wang, T. Van Voorhis, *J. Chem. Phys. Lett.* **2011**, *2*, 2200 – 2204.

[20] X. Li, P. E. Siegbahn, *J. Am. Chem. Soc.* **2013**, *135*, 13804 – 13813.

